Nucléation et cristallisation des matériaux vitreux

Comportement mécanique

J-C. Sangleboeuf LARMAUR ERL 6274

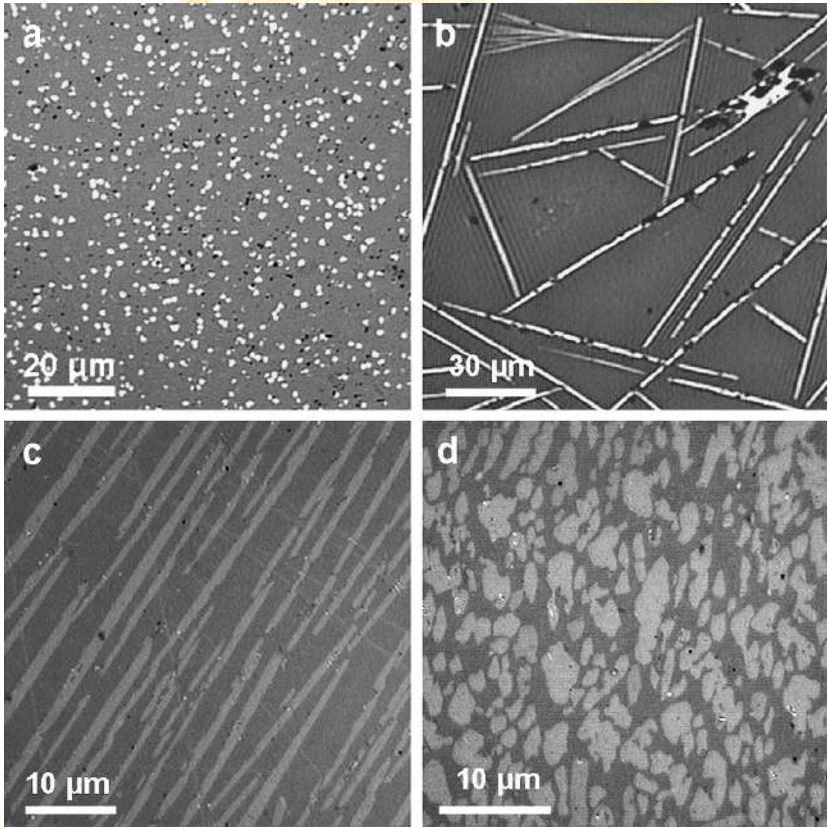

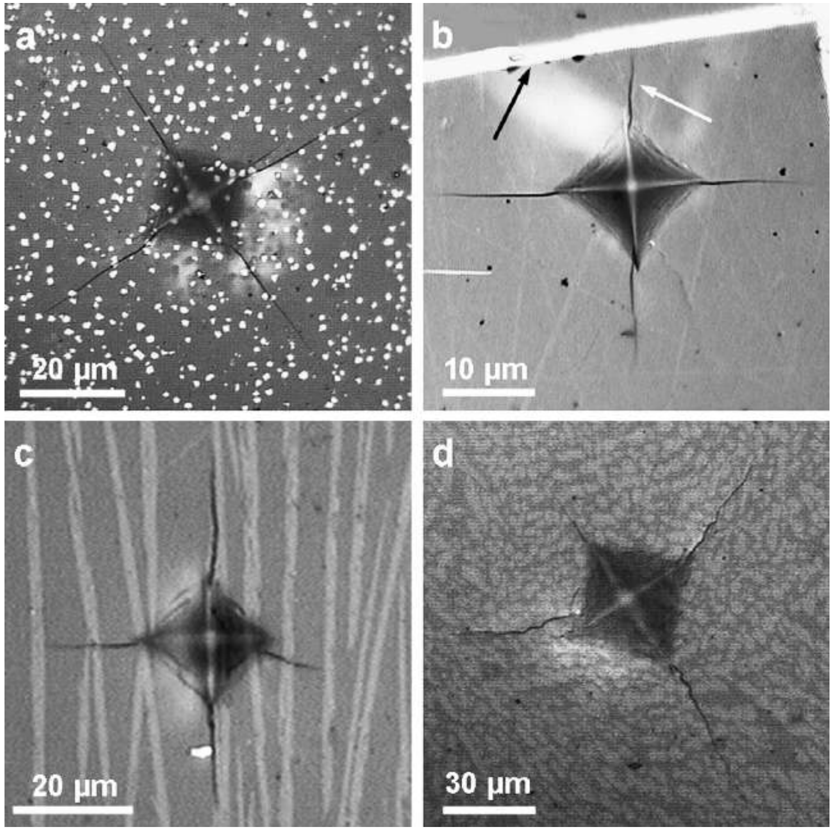

Kavouras et al JNCS (2006)

Nucléation – cristallisation - mécanique

1953 – S.D. Stookey – Corning Glass Works

Annealing of a lithium disilicate glass with silver particles.
He overheated the glass to about 900°C instead of 600°C
Instead of a melted pool of glass, the astonished Stookey observed a white material that had not changed shape.

He then accidently dropped the piece on the floor, but it did not shatter, contrary to what might normally have been expected from a piece of glass!
He was surprised by the unusal toughness of that material.

Stookey had accidently created the first glass-ceramic, denominated Fotoceram.

Adapted from Zanotto, Am. Ceram. Bul. Vol. 89, N°8, 2010

Sommaire

Mécanique des matériaux fragiles
- rappels
- propriétés et microstructure
- méthodes expérimentales

Cristallisation et élasticité

Cristallisation et résistance à la rupture – ténacité

-> à température ambiante

Mécanique Elastique Linéaire de la Rupture

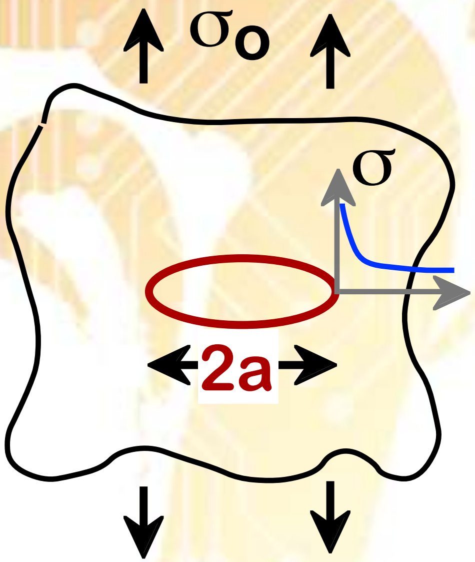

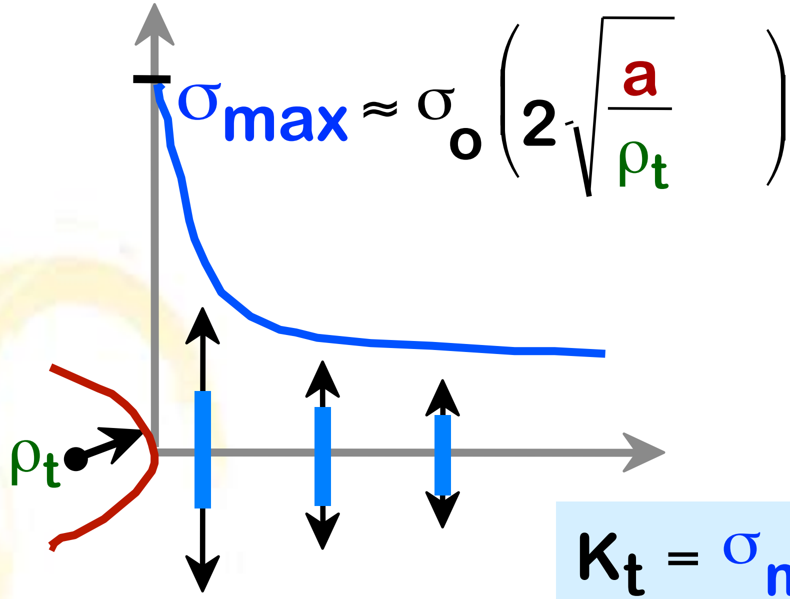

$K_t = \sigma_{max} / \sigma_o$

Griffith 1920s

$$\sigma_c = \left(\frac{2E\gamma_s}{\pi a} \right)^{1/2}$$

Irwin 1940s

$$\sigma_{ij} = \frac{K_I}{\sqrt{2\pi r}} f_{ij}(\theta) + \ldots$$

Facteur d'intensité de contrainte

$$K_i = Y \sigma_\infty \sqrt{\pi a}$$

K_{ic} = ténacité = résistance à la propagation de fissure

Ténacité et Indentation

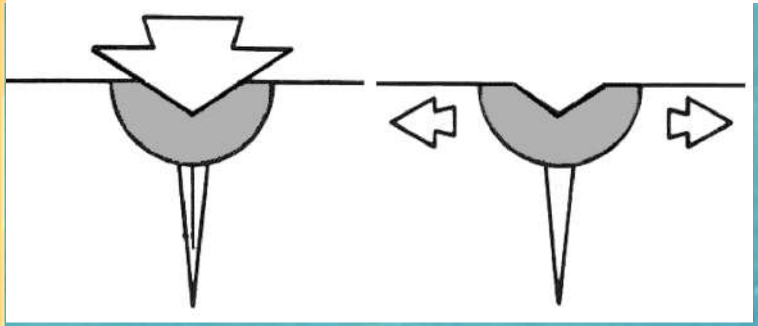

$$K_c = 0{,}016 \cdot \left(\frac{E}{H}\right)^{1/2} \cdot \frac{P}{c^{3/2}}$$

Marshall Lawn 1979

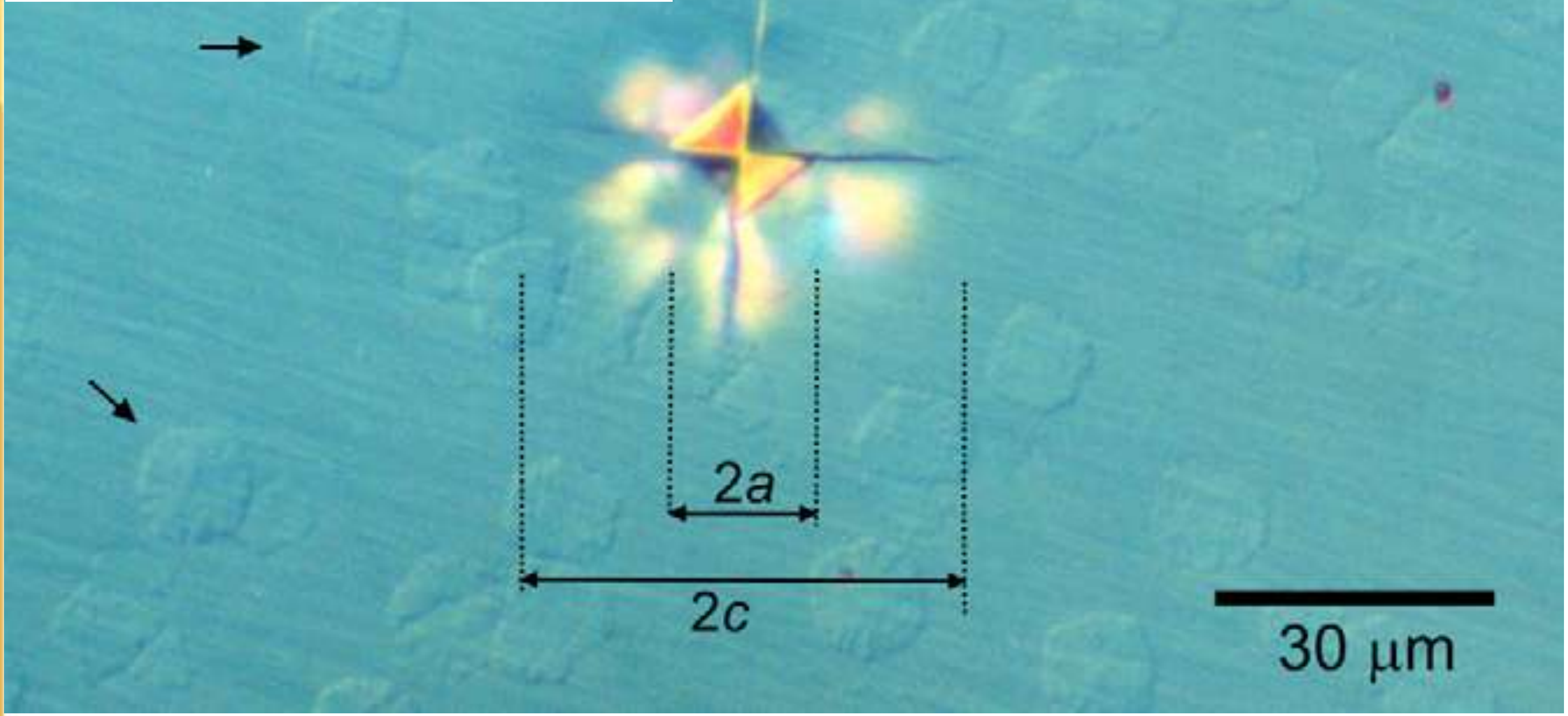

Peitl et al, Acta Biomaterialia 8 (2012) 321-332

Ténacité et poutres entaillées

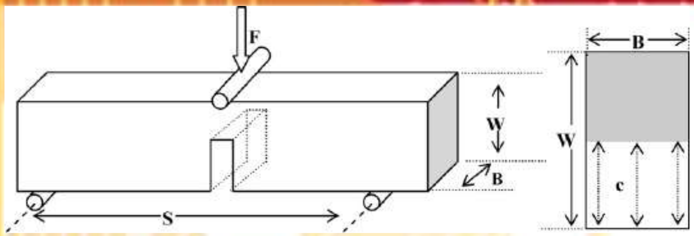

Single Edge Notched Beam->SEPB

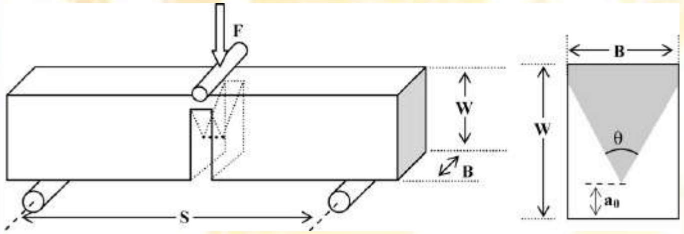

Chevron Notched Beam

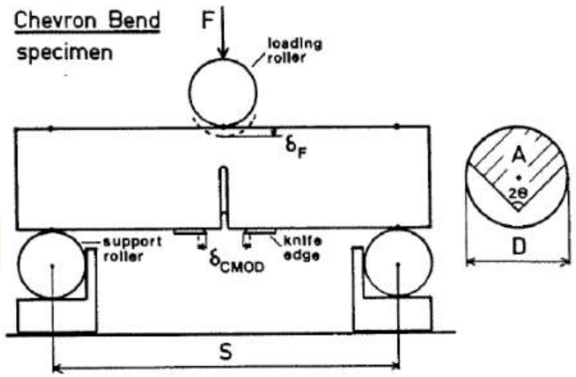

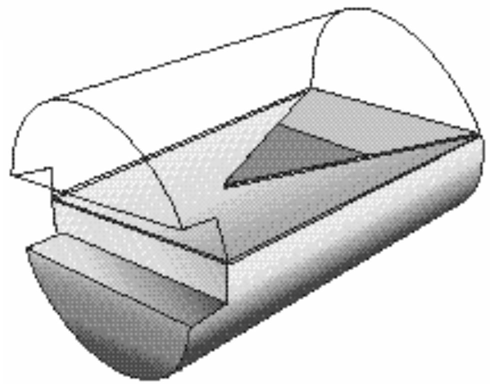

Short Rod Specimen

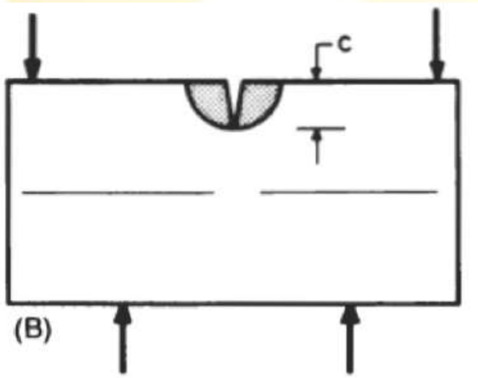

Indentation + 3PB-4PB-BF

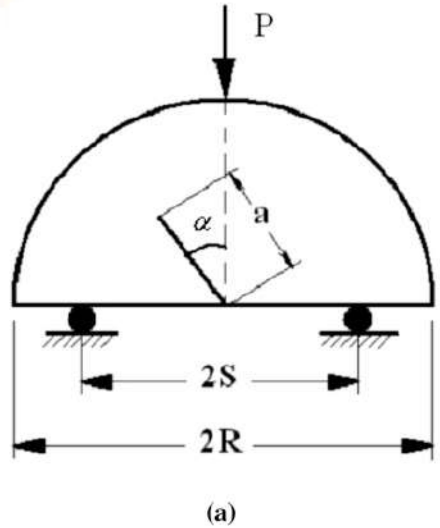

Semi Circular Beam

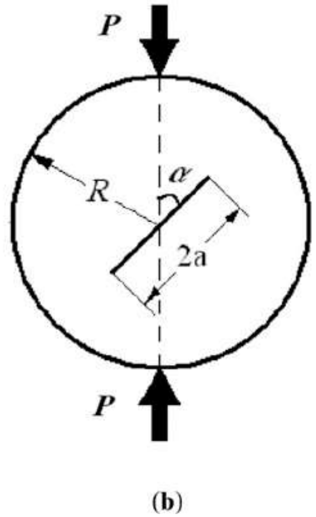

Centrally Cracked
Brazilian Disk

Cristallisation et Elasticité

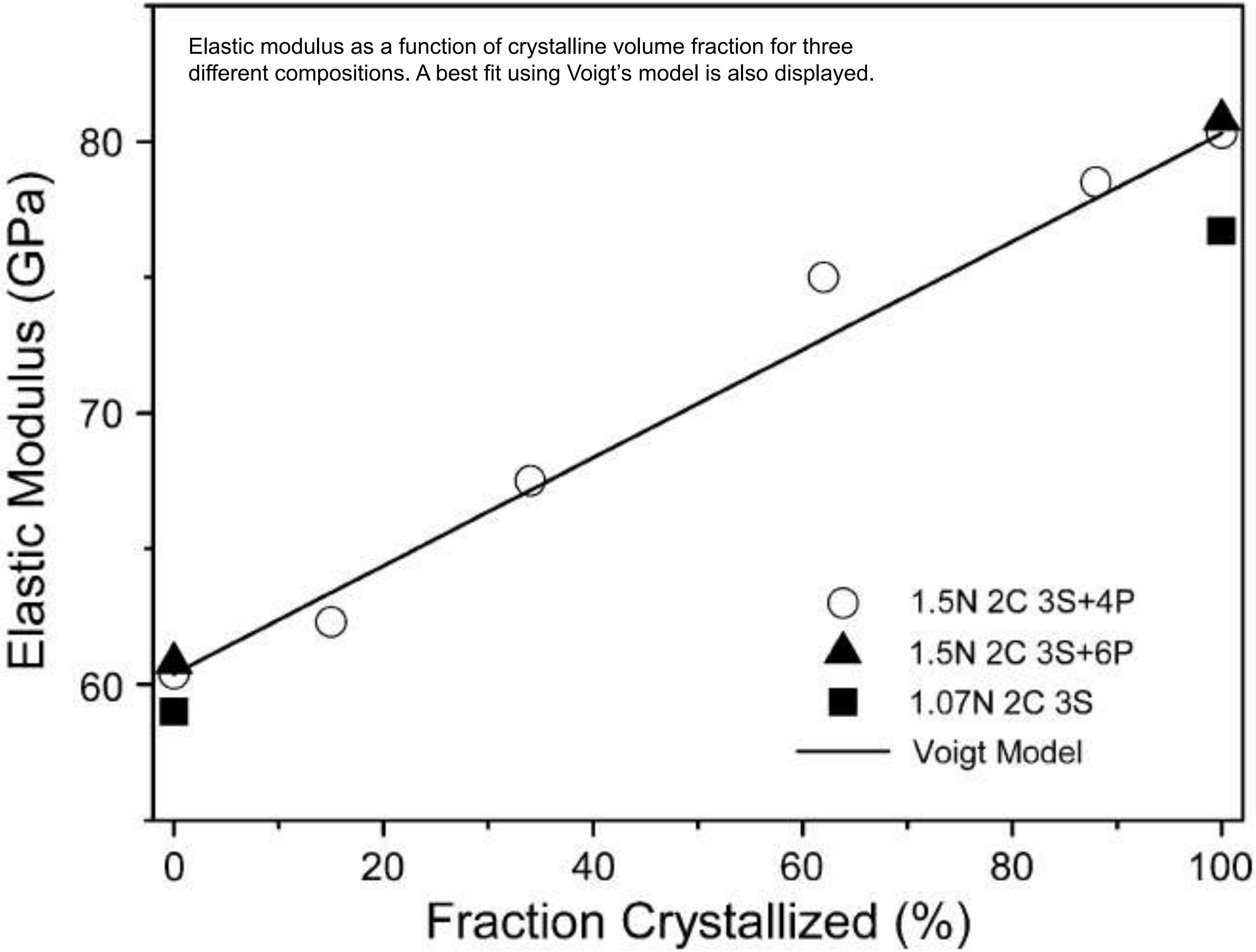

Peitl et al, Acta Biomaterialia 8 (2012) 321-332

Elasticité et modèle d'homogénéisation

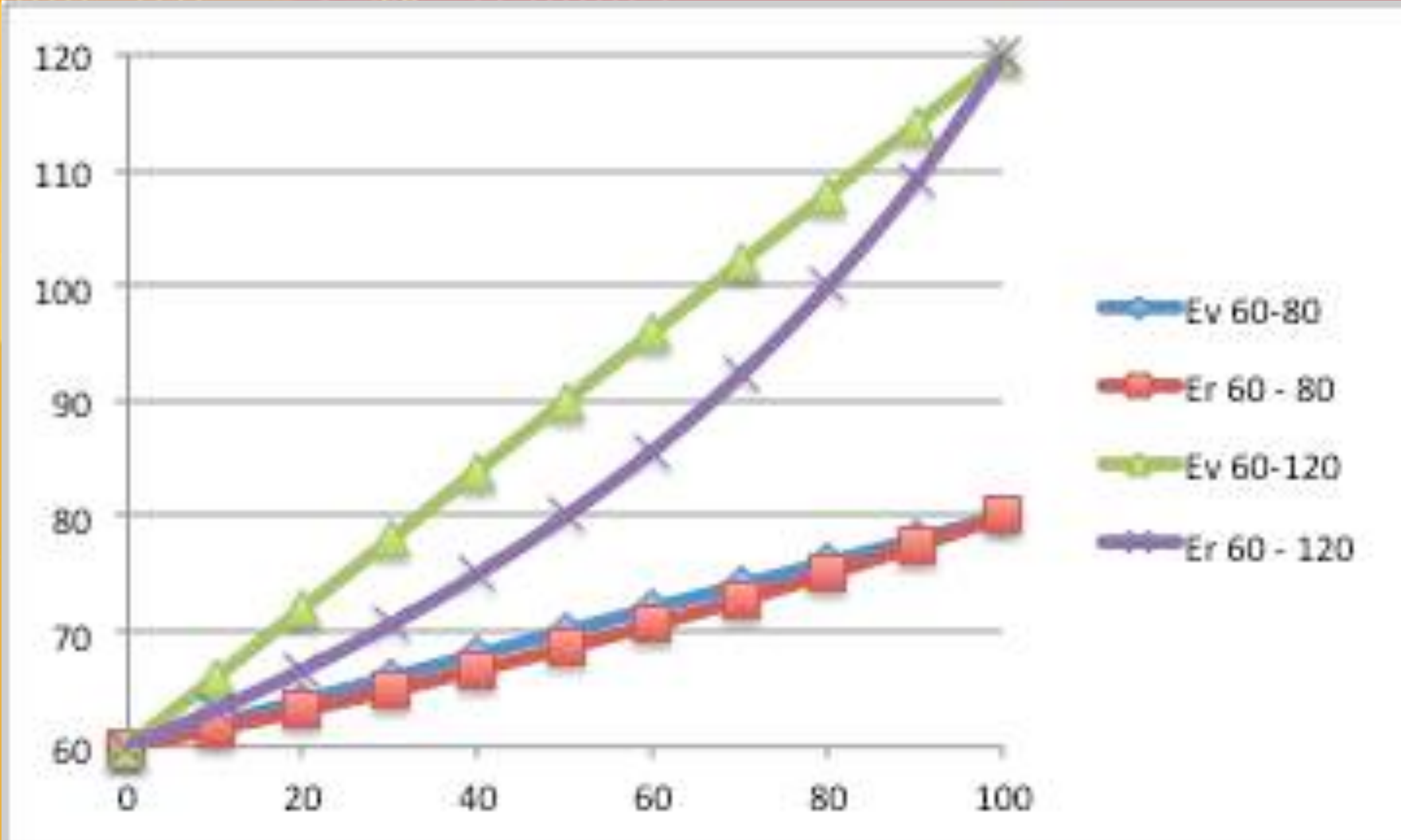

Importance du contraste mécanique

Propagation de fissure et microstructure

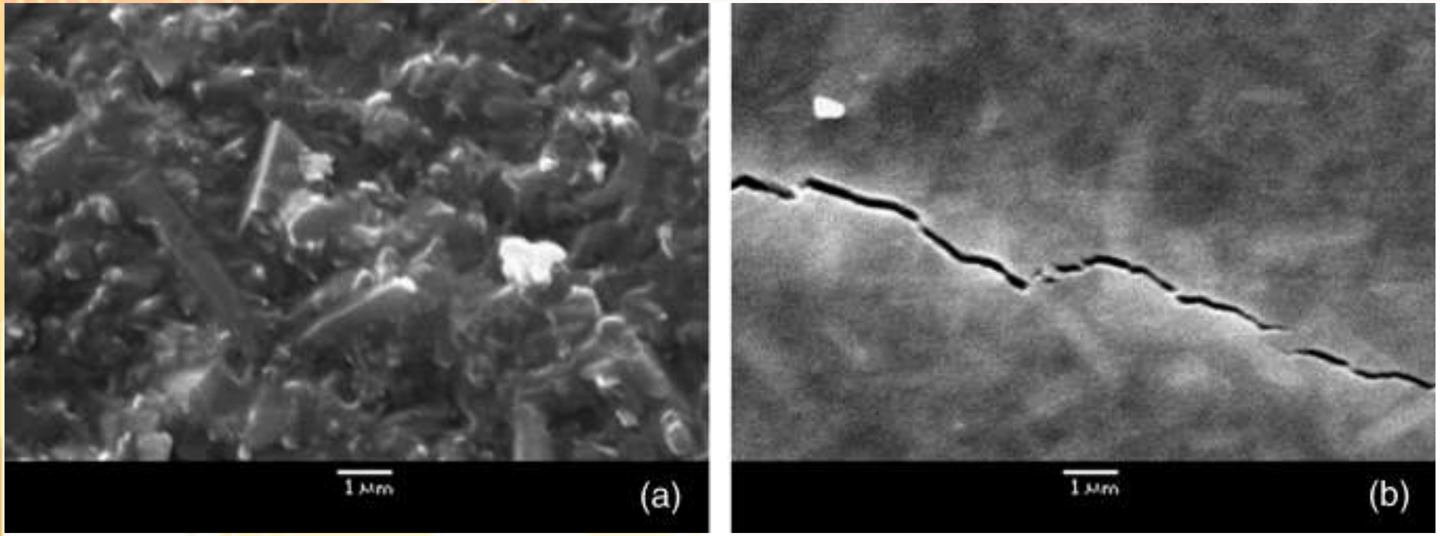

Micrographs showing (a) fracture surface of MS40G heat-treated at 1100°C for 2 h and (b) microscopic crack deflection across the material.

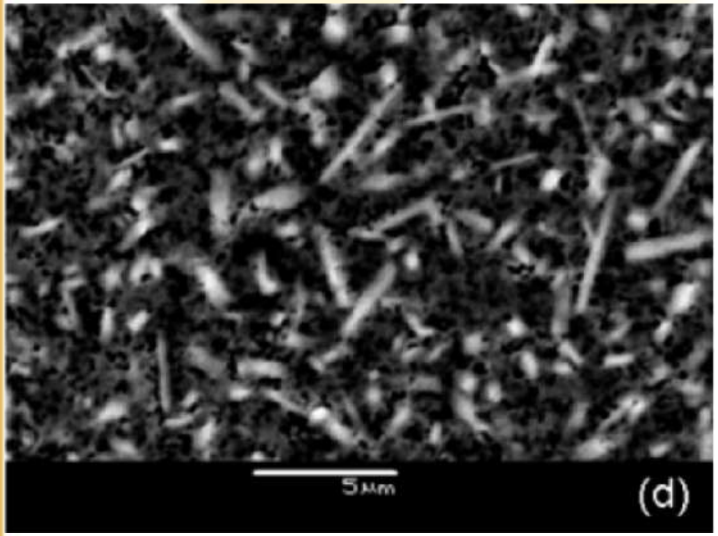

	As cast	HT 900°C	HT 110°C
K_{ind} MPa√m	0,9	1,0	1,6
BS MPa	101	134	184
CS MPa		500	700

Bending Strength
Compressive Strength

Wu JACS 2006

Propagation de fissure et microstructure

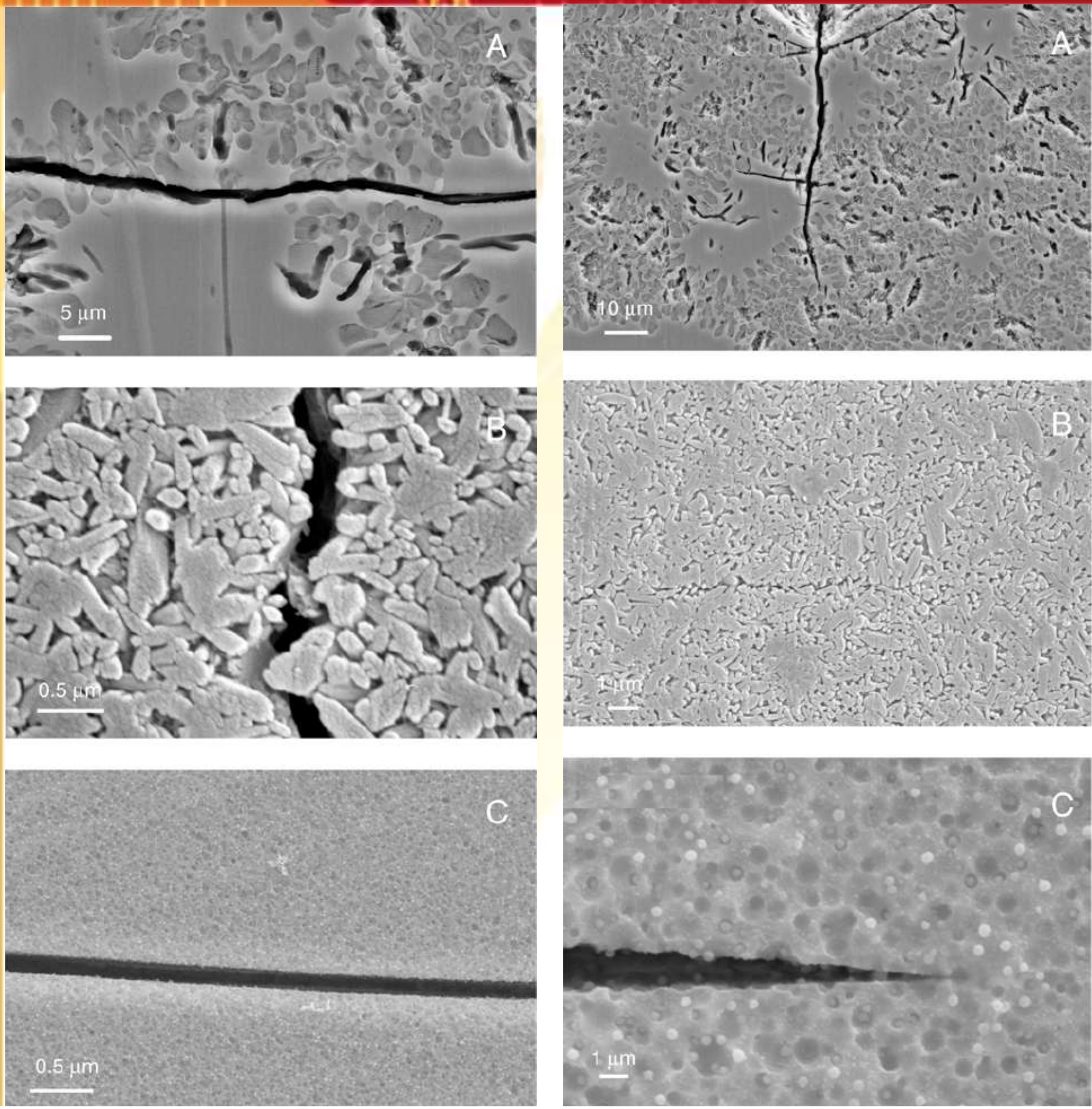

SEM images of the crack tips; the samples were etched with 3% hydrofluoric acid for 10 s;
(A) leucite glass ceramic
(B) lithium disilicate glass-ceramic
(C) apatite glass-ceramic.

	$K_{tip}d$ (MPa√m)	K_{SEVNB} (MPa√m)
A	0,55/0,58	1,09
B	1,28/1,19	2,7
C	0,58/0,60	0,7

Appel et al, J. Mech. Beh. Bio. Mater. 2008

Cristallisation et rupture

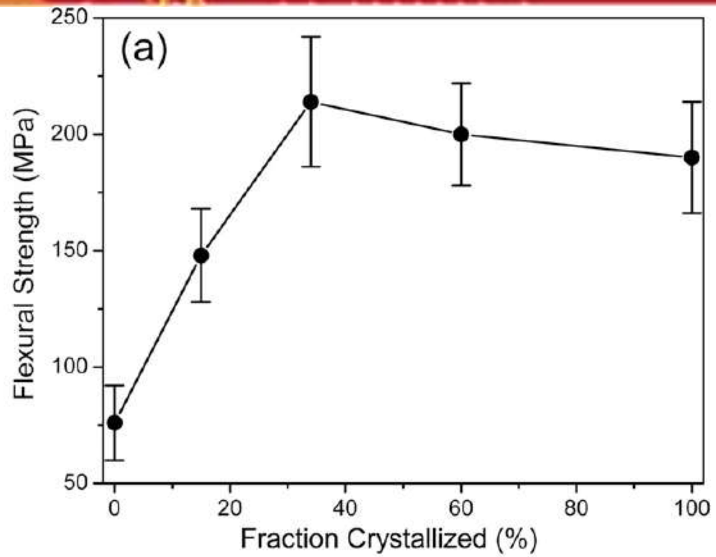

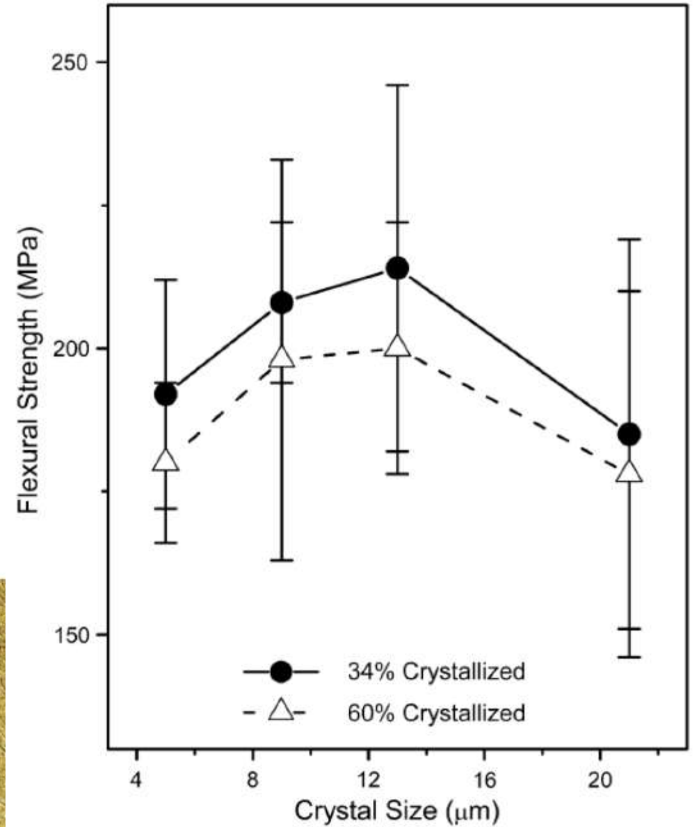

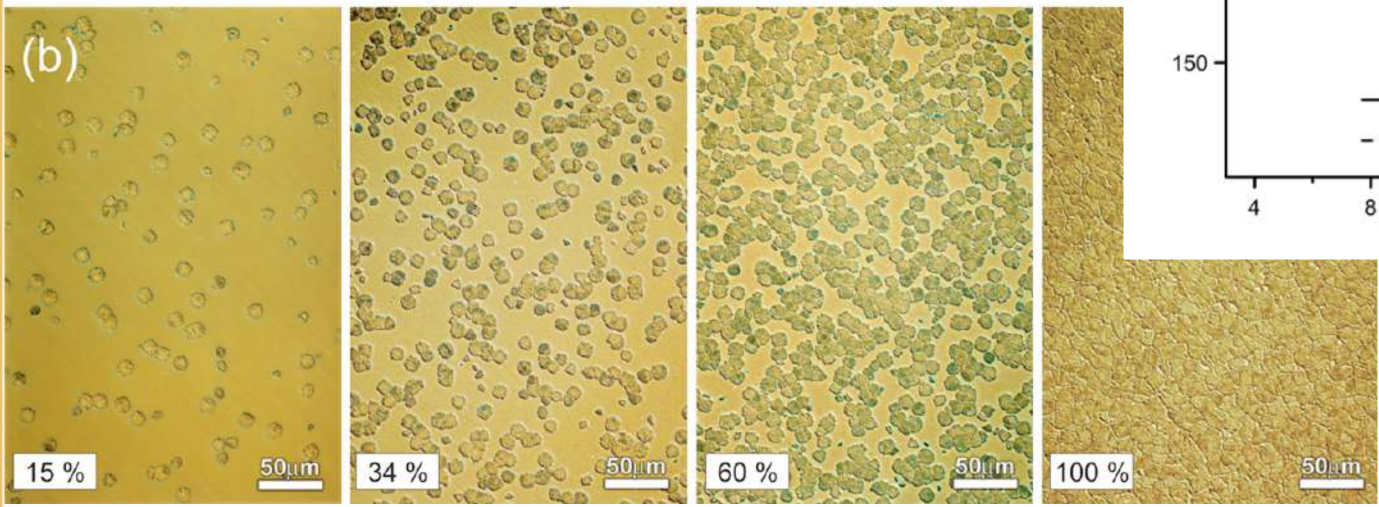

(a) Dependence of flexural strength on crystalline volume fraction for the 1.5N1.5C3S + 4P glass-ceramic with a constant 13 lm crystal size and (b) optical micrographs of the corresponding microstructures for 15%, 34%, 60% and fully crystallized samples.

Peitl et al, Acta Biomaterialia 8 (2012) 321-332

Cristallisation et rupture

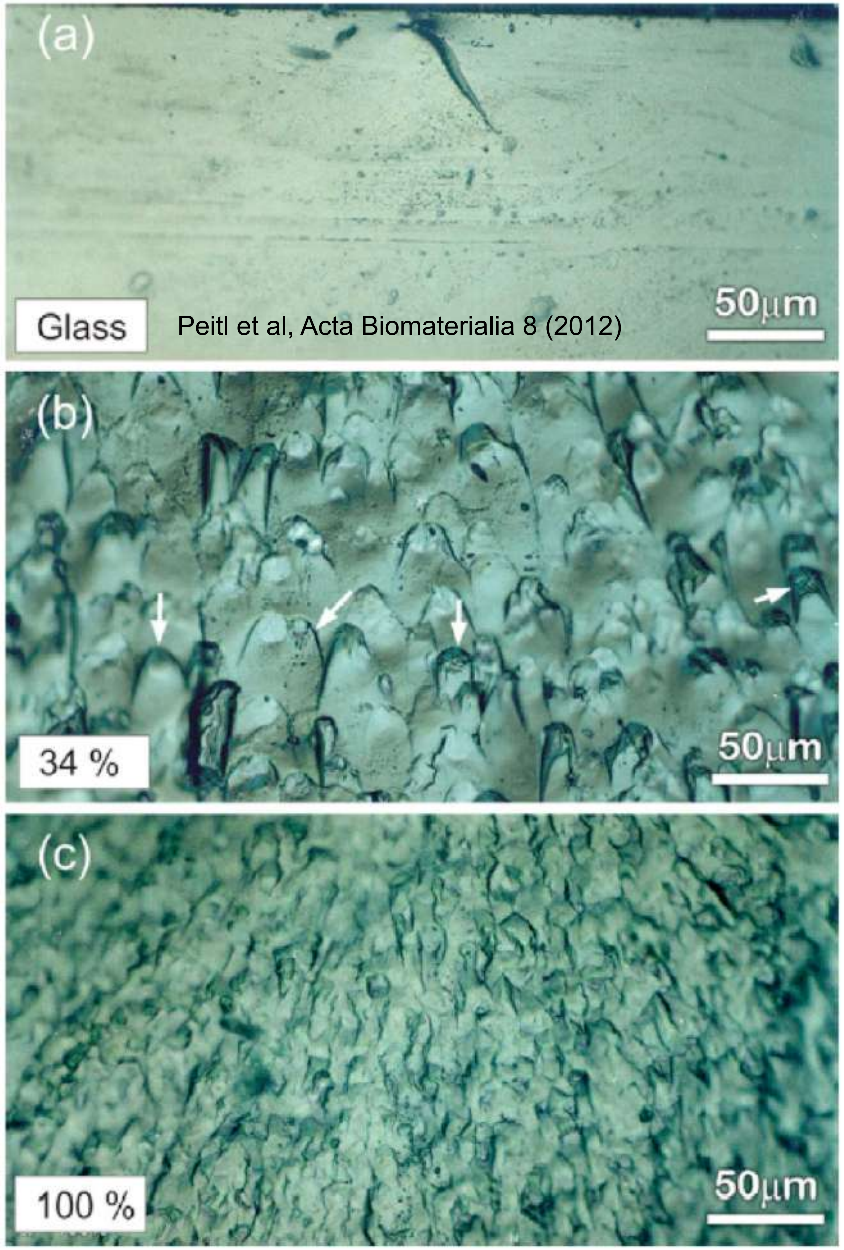

Peitl et al, Acta Biomaterialia 8 (2012)

Optical micrographs of the fracture surface of (a) glass and (b) 34% partially crystallized and (c) fully crystallized 1.5N1.5C3S + 4P glass-ceramic. Arrows in (b) show crack propagation in the glass matrix being deflected by crystals due to the radial tensile residual stress field.
Direction of fracture was from top to bottom.

Pontage?

Importance de :
- l'adhésion particule/matrice
- des α
- des E

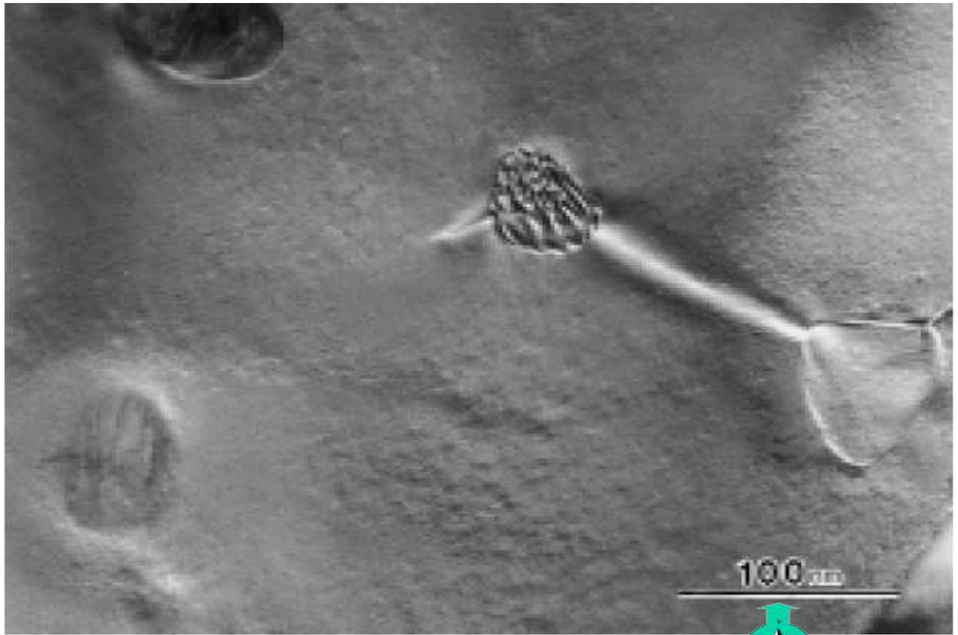

T Ohji et al JACS 1998

Rôle des contraintes résiduelles

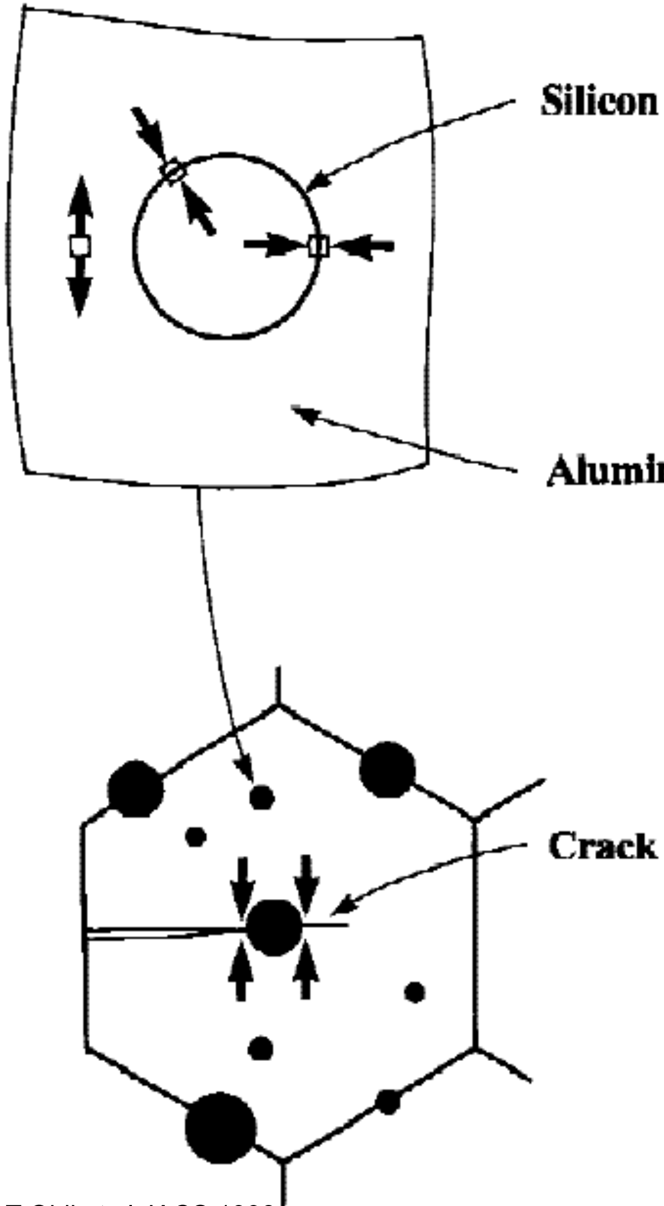

T Ohji et al JACS 1998

Inclusion sphérique, isotrope
Dans la matrice proche de
l'interface inclusion/matrice

$$\sigma_R = P = \Delta\alpha\Delta T / K_e$$

$$K_e = (1+\nu_m)/2E_m + (1-2\nu_p)/E_p$$

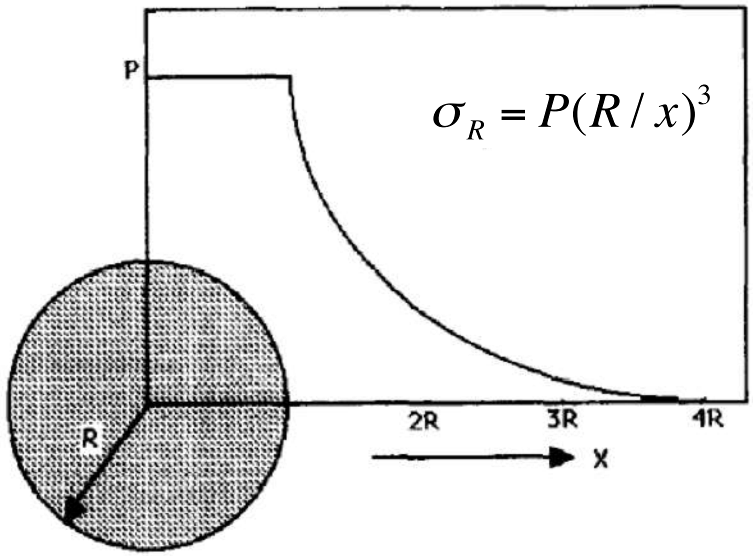

$$\Delta K = 2\sigma_m\sqrt{2\lambda/\pi}$$

Selsing JACS 1961

λ libre parcours moyen
ΔK ➚ si σ_m compression

Contrainte résiduelles et rupture

Crystallized phases, thermal expansion coefficient, bending strength and fracture toughness of glass-ceramics

Sample	Applied heat treatment/°C/h	Crystallized phases	Thermal expansion coefficient/K	Bending strength/MPa	Fracture toughness/MPa m$^{1/2}$
Z0	720/1 + 820/2	β-Quartz	0.4×10^{-7}	118	1.6
Z5	690/1 + 820/2	β-Quartz, β-Spodumene	0.9×10^{-7}	124	1.9
Z10	660/1 + 820/2	β-Quartz, β-spodumene, willemite	3.8×10^{-7}	135	2.1
Z15	620/1 + 820/2	β-Spodumene, willemite	5.3×10^{-7}	125	1.9

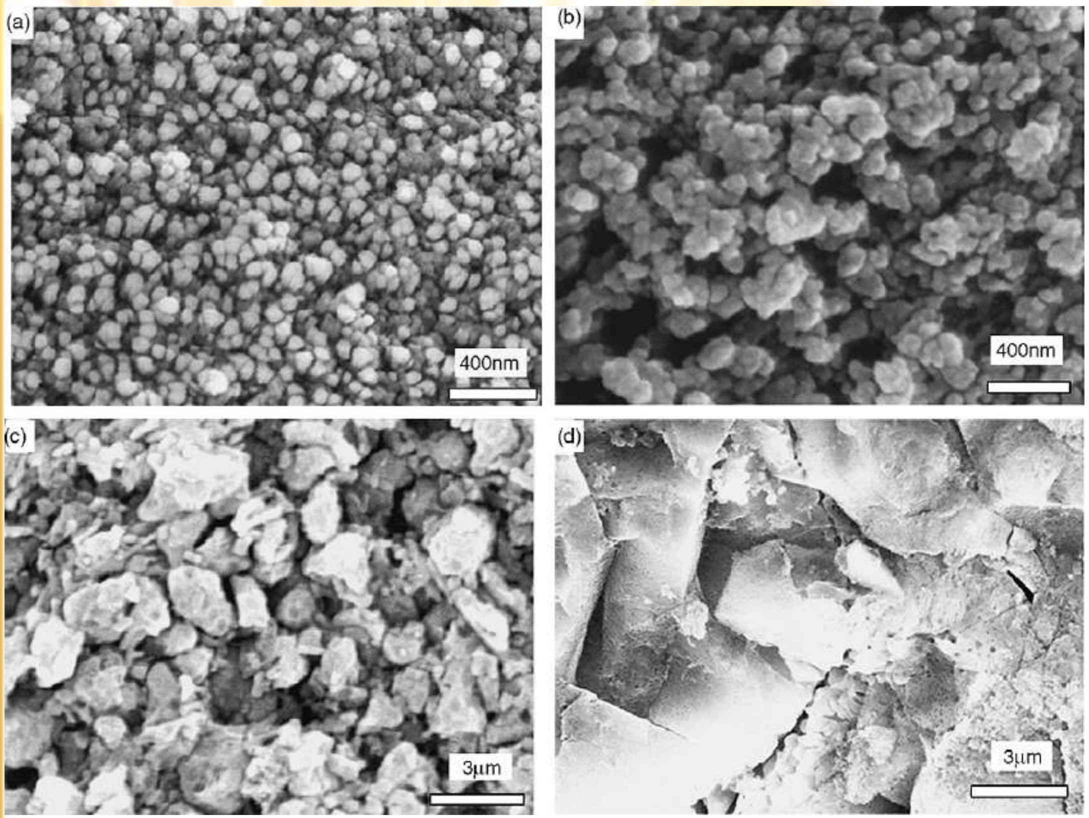

SEM photographs of Z0, Z5, Z10 and Z15 samples heat-treated at 820 °C for 2 h.

Hu et al, Thermochimica Acta (2005)

Substitution de Al_2O_3 par ZnO

βquartz $\alpha_q \approx$ 0-1.10^{-7}K^{-1}
βspodumène $\alpha_s \approx$ 9.10^{-7}K^{-1}
Willemite $\alpha_w \approx$ 15.10^{-7}K^{-1}

BS↗ car ↘σ_{res} internes liées au désaccord entre solution solide βquartz et matrice verre par précipitation βs et w.

Effet limité par la taille grain
Z0 Z5 100-200nm
Z10 1-2µm
Z15 3-5µm

Ténacité et cristallisation

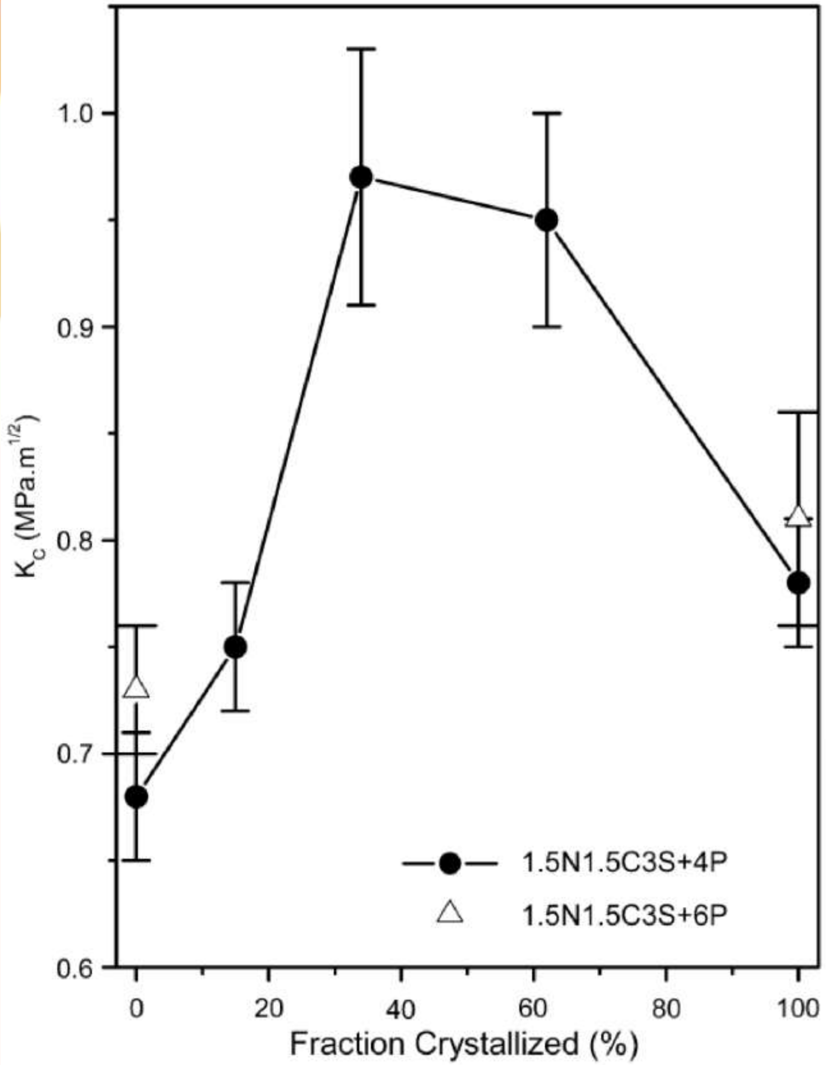

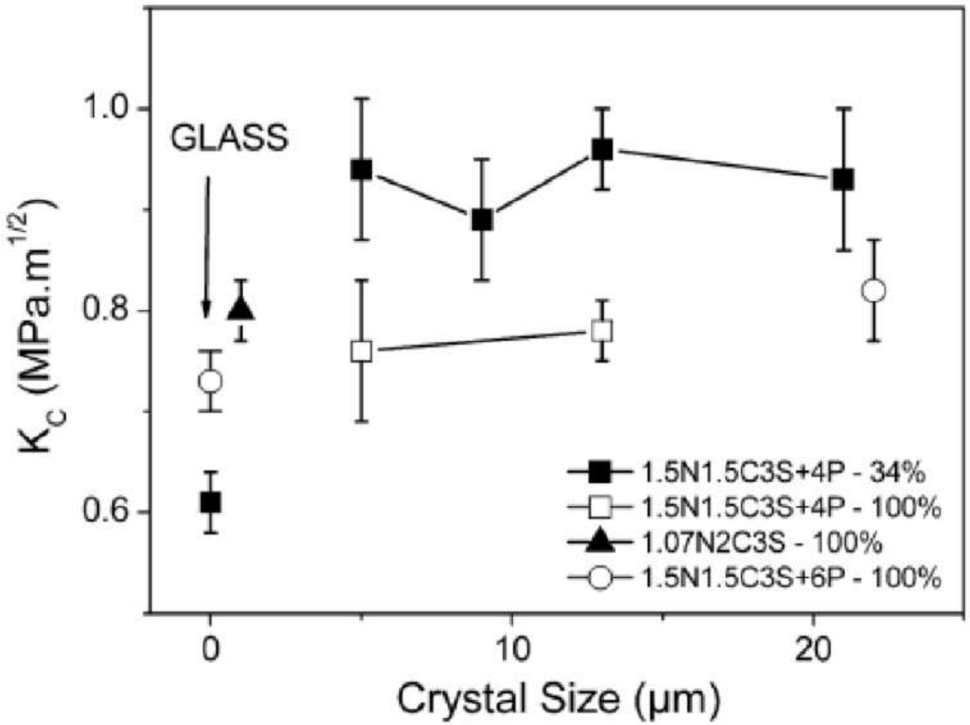

Influence de la distribution spatiale des cristaux

->λ

-> formation d'agrégats

->σ_{res}

Peitl et al, Acta Biomaterialia 8 (2012) 321-332

Ténacité et cristallisation

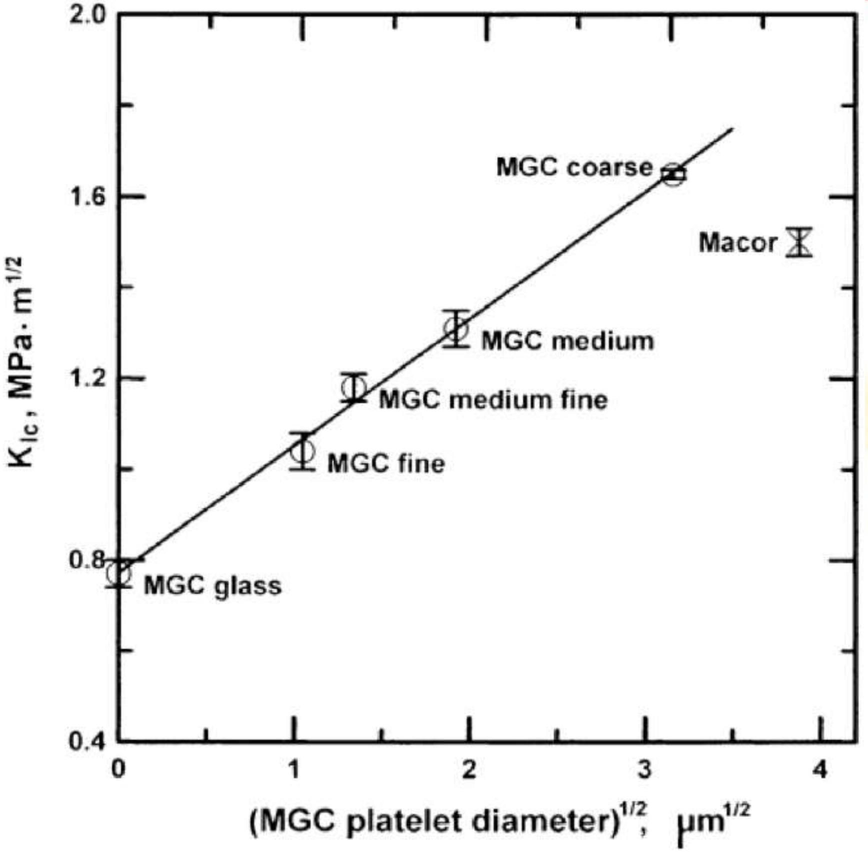

The increase of toughness with platelet size follows the square-root relationship predicted by the Becher model up to platelet diameters of about 10 mm (R^2 . 0.996). A drop in toughness is noted for Macor, with larger platelets and slightly different chemistry and microstructure.

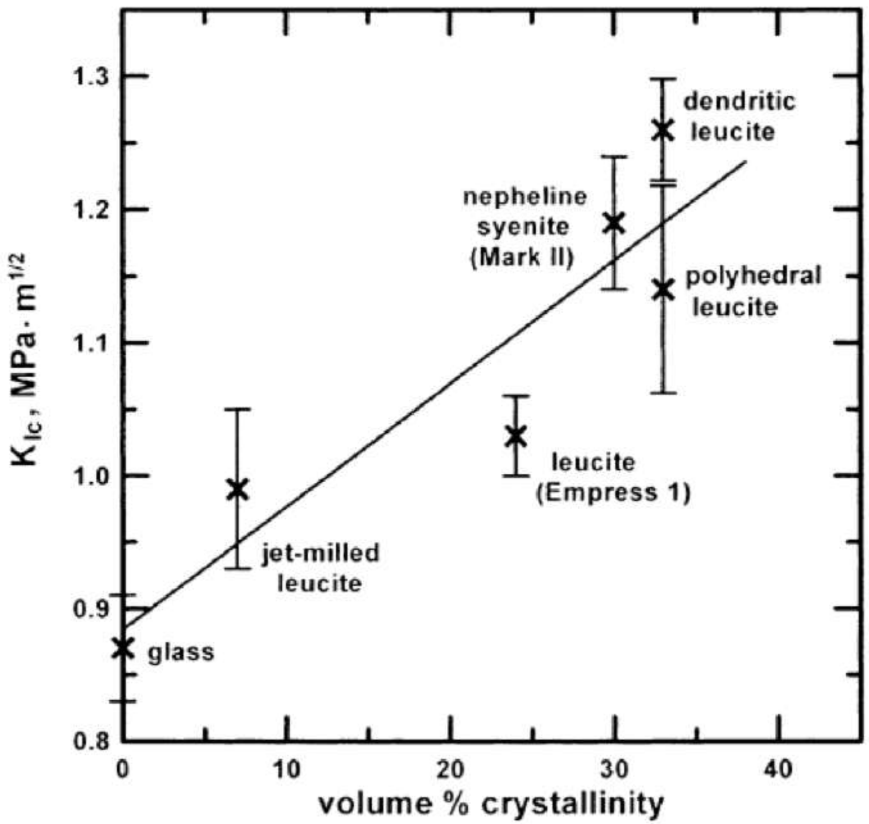

Toughness of the felspathic porcelains generally increases with %vol. crystallinity (R^2 . 0:845). Variations in chemistry, glass frits and microstructure contribute to scatter.

$$K_{Ic} = K_{Ic}^{(g)} + (A_{bg}\tau_f E d/2(1-\nu^2))^{1/2}$$

$K_{ic}^{(g)}$ is the fracture toughness of the base glass, A_{bg} is the areal fraction of bridging grains, τ_f is the frictional sliding stress, d is a grain size parameter, and E and ν are Young's modulus and Poisson's ratio.

Quinn et al, Dent. Mat. (2003)

Anisotropie et fissuration

Fracture toughness (K_{Ic}) of glass A extruded (or heat treated) at 824°C and subsequently crystallized at 1000°C for 30 min

Glass A	Oriented cut ∥ extr. axis center		Oriented cut ∥ extr. axis near surface		Oriented cut ⊥ extr. axis	Randomly oriented
Hardness H_V	3.8 ± 0.3		3.8 ± 0.3		3.7 ± 0.2	3.9 ± 0.1
Crack length (μm)	crack ⊥ 58 ± 3	crack ∥ 79 ± 8	crack ⊥ 44 ± 4	crack ∥ 120 ± 2	58 ± 4	69 ± 2
K_{Ic} (MPa $m^{1/2}$)	1.72 ± 0.21	0.77 ± 0.14	2.60 ± 0.46	0.57 ± 0.16	1.66 ± 0.25	1.32 ± 0.11

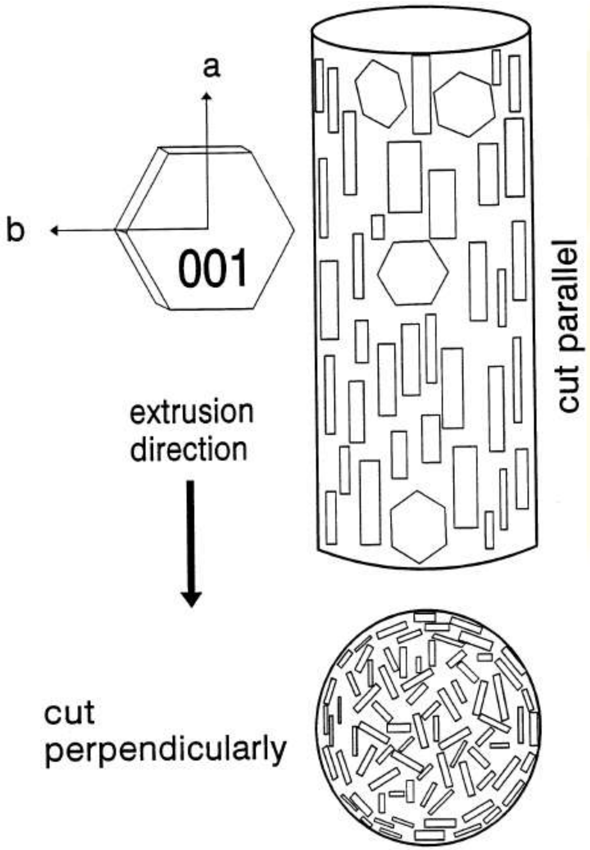

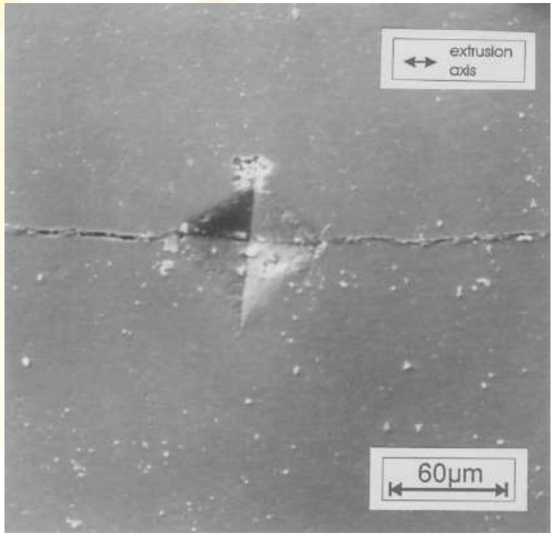

Vickers indentation on the surface area of oriented mica glass-ceramic of composition A, cut parallel to the extrusion direction.

Habelitz et al. Mat. Sc. Eng. A307 (2001)

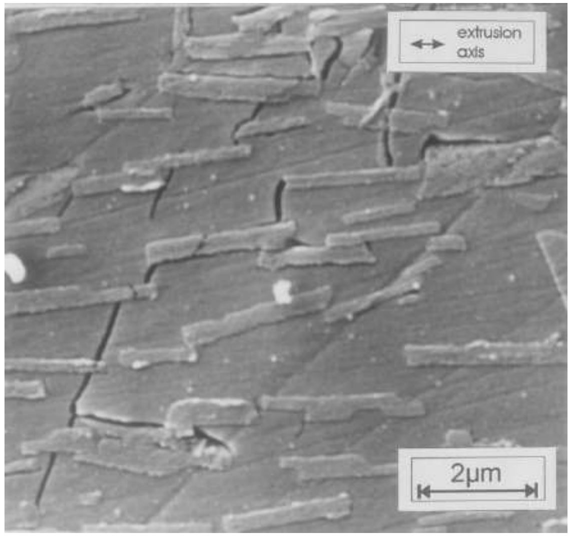

Deflected radial crack from Vickers indentation on the surface area of oriented mica glass-ceramic of composition A, sample cut parallel to the extrusion axis. Crack initiated perpendicular to the extrusion axis.

Extruded mica glass-ceramic

Anisotropie et fissuration

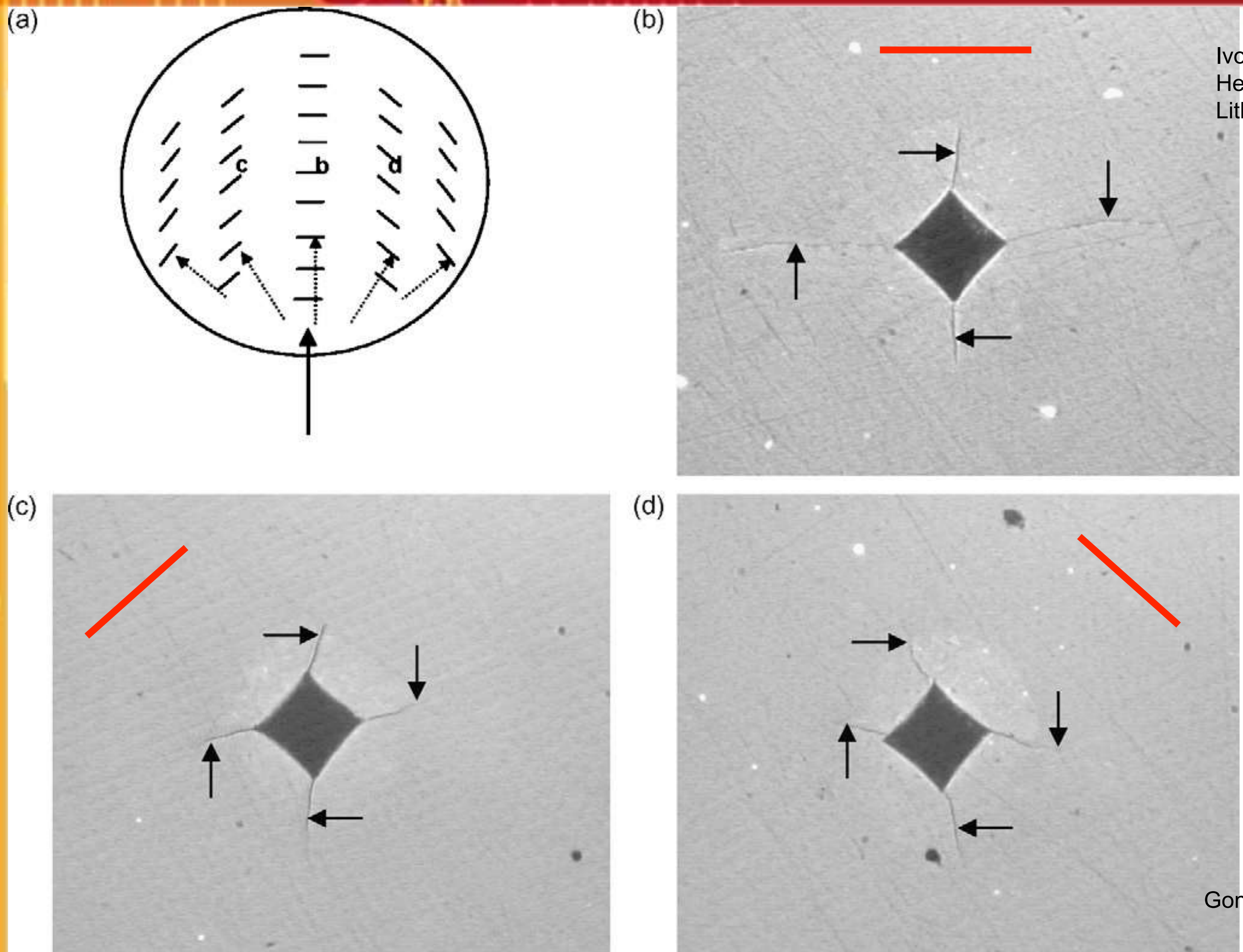

Ivoclar Vivadent/IPS Empress 2
Heta pressed
Lithium disilicate glass ceramic

Note the change in direction of radial cracks emanated from the impression corners.

Gonzaga et al, Dent. Mat. (2009)

(a) Schematic representation of the alignment of needle-like lithium disilicate particles in glass–ceramic E2 with disk-shaped specimen. The larger arrow indicates the direction of pressing and small arrows indicate the possible pressing force directions that resulted in particle alignment; (b–d) optical micrographs of the Vickers impressions made in the positions indicated with letters in (a).

Résumé

Elasticité et homogénéisation :
- Prise en compte de la morphologie
- Prise en compte de l'anisotropie

Fissuration – Rupture :
- Rôle important de la microstructure
- > déviation de fissure
- > défaut initial

- Rôle des contraintes résiduelles

- Rôle de l'anisotropie